Glass coated compressible solid oxide fuel cell seals

M. Rautanen*, O. Thomann, O. Himanen, J. Tallgren, J. Kiviaho

VTT Technical Research Centre of Finland, Fuel Cells, P.O. Box 1000, Biologinkuja 5, Espoo, FI-02044 VTT, Finland

HIGHLIGHTS

- A novel sealing material for solid oxide fuel cell stacks: conformable Thermiculite 866 core with thin glass coating.
- A method to coat thin glass layers using an organic carrier.
- Leak test results of glass coated seals.
- Stack test results using glass coated seals.

ARTICLE INFO

ABSTRACT

With the growing footprint of solid oxide fuel cell stacks, there is a need to extend the operating range of compressible gaskets towards lower stress levels. This article describes a method to manufacture SOFC seals by coating a compressible sealing material (Thermiculite 866) with glass to obtain good sealing performance even at compression stresses as low as 0.1 MPa. Glass layer can be coated using an organic carrier consisting of terpineol, ethanol and ethyl cellulose. The coated seals can be heat treated by simply ramping the temperature up to operating temperature at 60 Kh^{-1} and therefore no extra steps, which are typical to glass seals, are required. Coated seals were manufactured using this route and evaluated both ex-situ and in a real stack. Leak rates of 0.1–0.3 ml (m min)$^{-1}$ were measured at 2–25 mbar overpressure using 50/50 H$_2$/N$_2$. A 30-cell stack was manufactured and tested using coated seals. At nominal operating conditions of 0.25 A cm^{-2} and 650 °C average cathode temperature, 46% fuel utilization and 20% air utilization the stack had a total hydrogen cross leak of 60 ml min^{-1} corresponding to 0.7% of the inlet hydrogen flow rate.

1. Introduction

Traditionally solid oxide fuel cell (SOFC) stack seals have been either bonding seals (glass/glass-ceramic or brazes) or non-bonding (compressible) seals [1,2]. Bonding seals wet adjacent surfaces forming a very gas tight structure with little interfacial leakages. The usual drawback is that the bonding seals are susceptible to thermo-mechanical stresses especially in thermal cycling. Properties of glasses or glass-ceramics, such as coefficient of thermal expansion (CTE), viscosity and porosity, often change over time. During long term operation these changes can create additional thermo-mechanical stresses leading to seal failure [3,4]. Non-bonding compressible seals are more resistant to thermo-mechanical stresses as they are not rigidly bonded to adjacent components. However, their leak rates are usually higher and dominated by the interfacial leak paths, especially at low

compression stresses [5,6]. Compressible seals also require much higher compressive stresses compared to bonding seals, usually at least 2 MPa [7–9]. For example, in the results presented by Thomann et al. [10], with a cell footprint of 100 cm^2, the applied load on the stack was 2000 kg corresponding to roughly 4 MPa on the seals. If this stack was scaled up, the need for the applied load would naturally increase further complicating the mechanical design of the compression system.

Compressive stress is needed in SOFC stacks to ensure adequate sealing performance and to establish a good electrical contact between cells and interconnects. A general trend in SOFC stacks is towards larger cells and therefore towards larger stack footprints creating a need for higher compression on stacks, particularly the ones using compressible seals. This leads to heavier and more complicated compression systems. Compression rods usually need to go through the stack module heat insulation creating additional heat losses. Less compression would enable the use of thinner, less robust stack components. Therefore minimizing compressive stress required on the stack seals while maintaining the easy handling and assembly of the compressible seals would be beneficial.

* Corresponding author. Tel.: +358 405387552; fax: +358 207227048.
  E-mail address: markus.rautanen@vtt.fi (M. Rautanen).

In recent years, there has been some activity to develop composite seals combining properties from both compressible seals and glass-ceramic seals. The idea is to have a seal which would inherit its mechanical properties from the compressible core but, as opposed to standard compressive seals, would have very low interfacial leak rates because of the compliant surface coating. This would enable the compressible core to deform as a function of thermo-mechanical stresses without causing failure of the seal. Chou et al. have been experimenting with the hybrid sealing concept using different micas as substrates and glass or silver foil to seal the interfacial leak paths [5,6,11–15].

The hybrid seal developed at VTT Technical Research Centre of Finland is a composite structure consisting of compressible Thermiculite 866 [16] core coated with glass using an organic carrier. This method enables easy stack manufacturing as the seal can be coated beforehand and then cut and handled exactly in the same way as traditional compressible gaskets. The organic carrier is burned out in the first heat up and the remaining glass forms a thin conformable interlayer between the seal core and adjacent stack parts. The seal core is able to deform when subjected to stress and therefore can compensate e.g. differences in thermal expansion coefficients of adjacent components. A major advantage of the conformable core is also its ability to compensate for manufacturing tolerances of the adjacent components. Thermiculite 866 core is also less permeable compared to commonly used mica papers since voids between the platelets are filled with a fine grade of steatite. This paper presents a manufacturing method for the coated seals, ex-situ leakage test results and stack test results from a stack utilizing the sealing materials presented in this article.

2. Experimental

2.1. Seal manufacturing

Materials for the hybrid seals were chosen to target stack operation at around 700 °C. The chosen core material was Thermiculite 866 (Flexitallic Ltd) [16]. The glass layer was chosen to be relatively thin (<20 μm) so that the glass itself could be quite low in viscosity. The glass chosen for this study was a commercial glass material having a softening temperature of 650 °C.

Coating of the Thermiculite 866 seals was conducted using a mixture of glass powder and organic carrier. The organic carrier consisted of terpineol (mixture of isomers, Merck), ethanol (ETAX B, Altia) and ethyl cellulose (Fisher Scientific). Ethyl cellulose was mixed with terpineol and ethanol at 35 °C with a magnetic stirrer for 24 h. After that, glass powder was added and the mixture was stirred for 1 h. Table 1 presents typical compositions of the organic carriers and glass to organic ratios used in this study. When coating with brush/spatula/roller, a thicker coating paste proved easy to use and good coverage was achieved easily with a single layer. When using wet spraying, the carrier was diluted with more ethanol to achieve a lower viscosity of around 10–30 cSt which was suitable for the spray gun (U-POL Maximum HVLP mini with 1.0 mm nozzle). Several layers were sprayed from a distance of 10–20 cm.

After applying the coating, the coated Thermiculite 866 sheets were dried at 75 °C for 2 h and then cut to the required shape. All the seals were heated from room temperature up to 700 °C using 60 Kh^{-1} ramp rate.

2.2. Ex-situ leak tests

Ex-situ leak tests were conducted on ring-shaped seals having 40 mm outer diameter and 5 mm width. The seal was placed on top of 20 mm thick Crofer 22 H (Thyssenkrupp VDM) plate. A 1 mm thick Crofer 22 H plate was placed on top of it and weight plates on top of the 1 mm plate. Gas was fed to the middle of the seal through the thick bottom plate. Fig. 1 presents the experimental setup for ex-situ leak rate measurements. Mass flow controllers fed a chosen gas mixture to the sample line and exhaust line. Sample pressure was controlled with a pressure controller which vents a sufficient flow of gas to the exhaust to keep the upstream pressure at a set level. During heat up, air was fed to the samples to ensure a complete organic burn off.

After heat up, samples were exposed to a 25 mbar overpressure using 50/50 mix of H_2/N_2 at 700 °C. Periodical leak rate measurements were conducted by shutting off the valve V 1 and measuring the pressure decay. A vessel of a known volume was connected to the sample enabling leak rate as a function of pressure to be calculated from the pressure decay curve. Based on the ideal gas assumption, the leak rate is proportional to the slope of the pressure decay curve and therefore the leak rate can be written

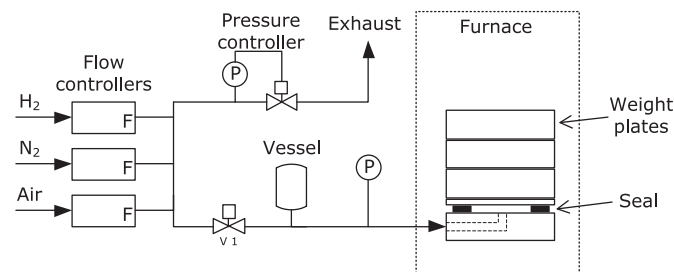$$\dot{Q} = V \frac{T_{ntp}}{Tp_{ntp}} \frac{dp}{dt},$$

where V is the combined volume of the vessel and the sample, T is the average temperature of the gas in the volume and T_{ntp} and p_{ntp} are normal temperature and pressure. To calculate the leak rate one needs to evaluate dp/dt over the measurement data. If one wants to calculate leak rate at a specific pressure from the data which is a set of points taken at regular intervals, one could approximate dp/dt by

$$\frac{dp}{dt} \cong \frac{p_i - p_{i-1}}{t_i - t_{i-1}}.$$

If the sampling rate has been sufficient, the difference $p_i - p_{i-1}$ is bound to be small. As the uncertainty of dp/dt is proportional the uncertainty of the pressure measurement

$$\varepsilon \left(\frac{dp}{dt} \right) \propto 2\varepsilon(p),$$

this approach would yield very inaccurate results. To overcome this, a third degree polynomial was fitted to the $p(t) -$ data using least squares method thus minimizing the random uncertainty of the $p(t)$ measurement. Goodness of the fits were analyzed by calculating relative standard deviation of residuals and in case those were over

Table 1
Typical composition of organic carrier and glass to organic ratio with different coating methods.

Coating method	Terpineol/w%	Ethanol/w%	Ethyl cellulose/w%	Glass to organic ratio/w/w
Brush/spatula/roller	81	15	4	2:1
Wet spraying	24	75	1	1:2

Fig. 1. Measurement setup for the ex-situ leak rate test. Four samples were tested simultaneously, although in here only one is shown for clarity.

Fig. 2. The 30-cell stack before testing.

1.0% fits were discarded. The fitted polynomial was then differentiated to obtain leak rate as a function of pressure. As the accuracy of the pressure transducer is very good (± 0.5 mbar) it can be concluded that the accuracy of the pressure measurement has negligible effect on the results. The accuracy of the gas temperature measurement was $\pm 15\,^\circ$C corresponding to a leak rate uncertainty of 5%.

Quantifying leak rate using the pressure decay methodology described above offers the advantage of relatively simple measurement which can be easily automated. The disadvantage of the method is that by using it one only measures leak rate indirectly by measuring the pressure inside the volume, which is dependent on the flow rates of species through the seal boundary. By using other gas than air, there is always a concentration difference over the seal and therefore also a flux of species from outside to inside by diffusion, which has an effect on the observed flow rate.

2.3. Stack test

In addition to the ex-situ tests, a 30-cell stack was manufactured and tested together with Elcogen. The stack utilized Elcogen ASC-10B cells and ferritic steel interconnects. The seals were made of coated Thermiculite 866 except for the seal against the electrolyte which was made of glass, as it needed to be thinner than the thinnest coated seal that was achievable at the time the work was carried out. Fig. 2 shows the 30-cell stack in a furnace before testing. The compression on the stack was provided through a pipe seen at the upper end of the picture. Pipe coils seen at the bottom of

the furnace acted as pre-heaters for air and fuel. On the right side of the picture current collectors attaching to the end plates are seen. Pipelines to measure stack pressures are seen to exit the furnace to the left. The stack was heated up using air flow at both anode and cathode. After reaching the operating temperature, nitrogen was fed to the anode side and afterwards reduction was carried out with hydrogen in nitrogen mixture. During stack polarization, hydrogen and air flows were increased while increasing current and nitrogen flow was kept constant at 8.5 NLPM.

Cross leakages were quantified by measuring steam and oxygen content from cathode and anode outlets. Steam was measured with Vaisala Humicap HMT-337 relative humidity meter ($\pm 1\%$ RH) and oxygen with Sick TRANSIC100LP ($\pm 0.2\%$ − units O_2). Zero level of the oxygen probe was calibrated with nitrogen and the accuracy was determined to be 0.05% − units below 1% O_2. Oxygen cross leak was calculated before reduction as

$$\dot{Q}_{O_2}^{\text{cross}} = X_{O_2}^{A,\text{out}} \dot{Q}_{N_2}^{A,\text{in}}$$

The hydrogen cross leak after reduction was calculated as

$$\dot{Q}_{H_2}^{\text{cross}} = \left(X_{H_2O}^{C,\text{out}} - X_{H_2O}^{C,\text{in}} \right) \left(\dot{Q}_{\text{air}}^{C,\text{in}} - n_{\text{cells}} \frac{I}{4F} \frac{RT_{\text{ntp}}}{p_{\text{ntp}}} \right),$$

where terms denoted with X are measured oxygen and steam volumetric fractions, n_{cells} is the number of cells in the stack (30), I is the current drawn from the stack and F is the Faradic constant. These calculations are based on the assumption that the leak rates between ambient and anode/cathode and the nitrogen cross leak are small compared to total flow rates.

3. Results and discussion

3.1. Seal manufacturing

Samples for the SEM analysis were cut out of coated Thermiculite 866 sheets and placed between two 1 mm Crofer 22 H sheets. The samples underwent a heat treatment described in Section 2.1 with a 50 h dwell at 700 $^\circ$C. Fig. 3 shows SEM cross sections of the prepared samples. The horizontal platelets in the Thermiculite 866 are exfoliated vermiculite and the filler between them is steatite. The figure shows the advantage of this material over conventional mica papers as the inherent voids in the flaky mica structure are filled with steatite and therefore the gas tightness is improved. The compressibility of this material is also superior to conventional mica papers [9]. Thin glass layers of 2–10 μm are seen at the interfaces of Thermiculite 866 and Crofer 22 H plates. It can be noted that the glass has accommodated very well to the surface roughness of the Thermiculite 866 and even penetrated into its
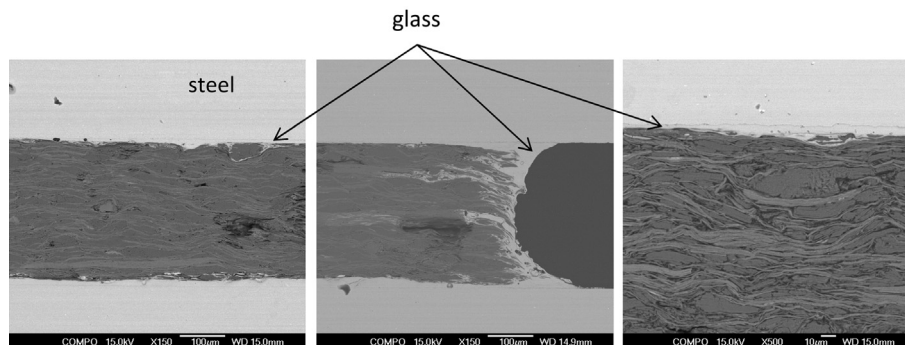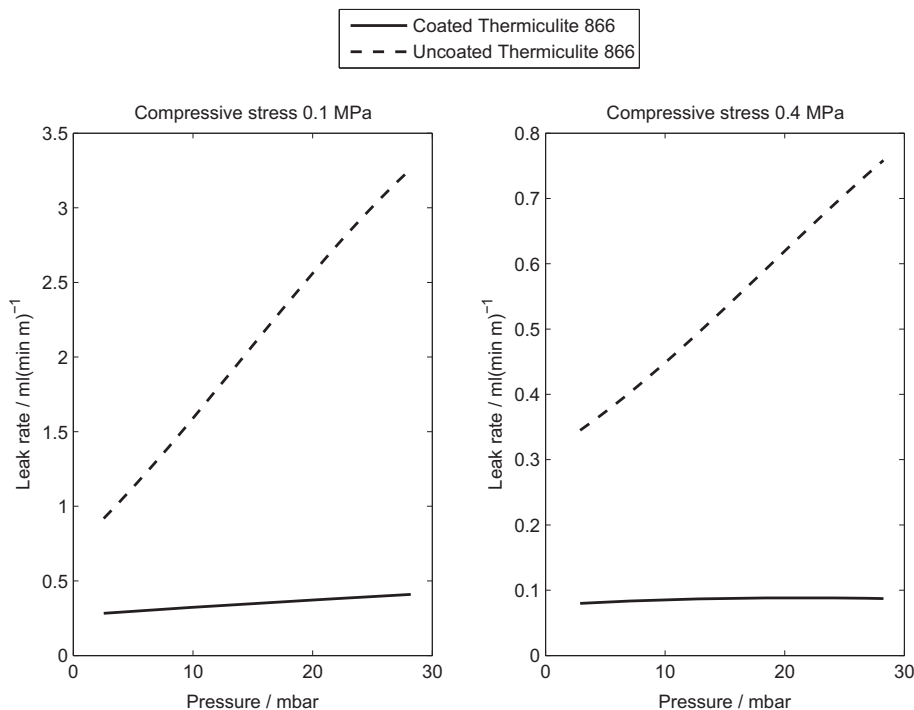

Fig. 3. SEM cross sections of the coated seals. From left to right: middle section of the seal, end of the seal and close up of the steel/glass/Thermiculite 866 interface.

Fig. 4. Leak rates of coated and uncoated Thermiculite 866 at compressive stress of 0.1 MPa (left) and 0.4 MPa (right) with 50/50H$_2$/N$_2$. Note the different scales of the vertical axes.

pores. The low initial viscosity of the glass layer provides good conformability to the Thermiculite 866 core and to any surface imperfections on the adjacent components.

3.2. Ex-situ leak tests

Fig. 4 presents leak rates of the samples as a function of pressure at 0.1 MPa and 0.4 MPa compressive stress. From this figure it can be noticed that the surface coating decreases the leak rate of Thermiculite 866, especially at low compression stress levels. The coated Thermiculite 866 seals show leak rates of 0.1–0.3 ml (m min)$^{-1}$, which is a reduction of 60–90% compared to uncoated samples which showed leak rates of 0.3–3 ml (m min)$^{-1}$. Chou et al. have measured leak rates below 1 ml (m min)$^{-1}$ using

mica papers with glass interlayers at compressive stresses of 0.04–0.7 MPa and less than 0.1 ml (m min)$^{-1}$ using glass sealing [5,12,15,17]. The tests have been carried out either with helium or 2.64% H$_2$ in humidified Ar. Although different conditions make direct comparison difficult, it is clear that the results presented in this paper are at a comparable level to the hybrid seals developed by Chou et al.

Fig. 5 presents leak rates of coated and uncoated Thermiculite 866 with different gas compositions and overpressures. The leak rate of the uncoated sample clearly depends on both overpressure and the hydrogen concentration but the leak rate of the coated sample only depends on the hydrogen concentration. As the driving potentials, overpressure and concentration gradients, are same for both measurements, it can be concluded that the coating effectively
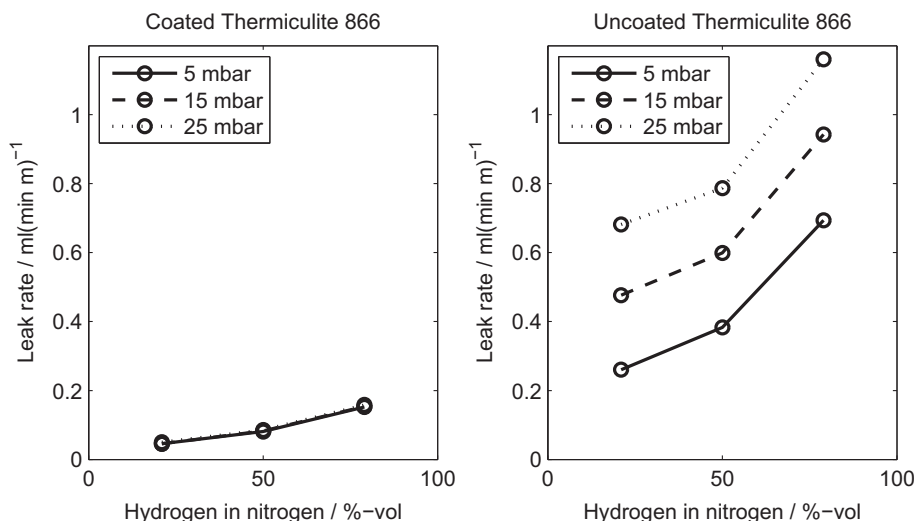
Fig. 5. Leak rates of coated (left) and uncoated (right) Thermiculite 866 at different overpressures as a function of hydrogen concentration. Compressive stress is 0.4 MPa.
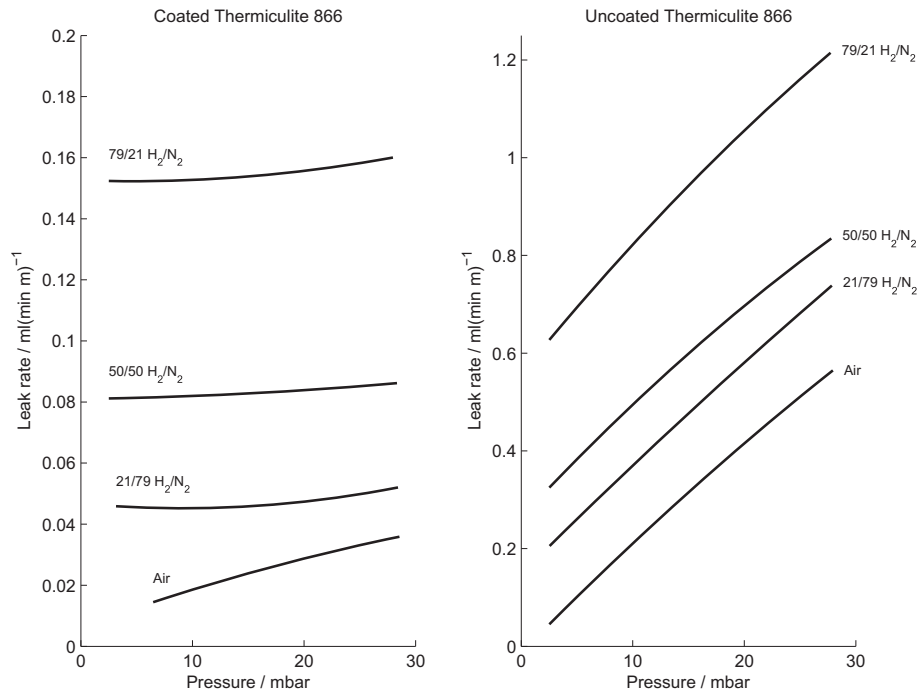
Fig. 6. Leak rates of coated (left) and uncoated (right) Thermiculite 866 as a function of overpressure with 0.4 MPa compression stress with different gas compositions.

blocks the direct leak paths and the remaining leak rate is due to diffusion rather than advection. This is further shown by looking at the curves measured with air (Fig. 6). Extrapolating the curves one obtains a zero leak rate at zero pressure difference when other gas compositions yield a non-zero leak rate also at zero pressure difference. The negligible dependency of the overpressure on the diffusive leak rate can understood by considering Fick's law of diffusion written for a component A using total concentration c_{TOT} total pressure p_{TOT} and the molar fraction x_A:

$$J_A = -D_{AB}\nabla c_A = -C_{TOT}D_{AB}\nabla x_A = -\frac{p_{TOT}}{RT}D_{AB}\nabla x_A.$$

From this equation one can notice that varying the absolute overpressure p_{TOT} in a range of $\sim 1000–1030$ mbar induces very little effect on the concentration driven leak rate. Although the real situation is more complex, the concentration dependency of the leak rates should be carefully considered as different research groups use very different gas compositions and overpressures for leak tests, such as 3% H_2 in nitrogen or argon, 100% H_2 or 100% He.

3.3. Stack test

Hydrogen cross leak was measured with purge gas and at nominal operating conditions (Table 2). Table 3 shows stack flows,

measured values and the calculated cross leaks at different operating conditions. The air inlet humidity was constant 0.08%. Before reduction, the O_2 cross leak was 8 ml min^{-1}. After reduction the H_2 leak rate using purge gas was 10 ml min^{-1} and 60 ml min^{-1} at nominal operating conditions. Fig. 7 shows the hydrogen cross leak as a function of average hydrogen concentration between anode inlet and outlet during the test. The concentration dependency of the leak rate can be clearly noticed as in the ex-situ tests. During nominal operating conditions the overpressure at cathode was higher than the pressure at anode and therefore the measured hydrogen leak is against the pressure gradient which suggests that the remaining leak rate is due to diffusion rather than advection through the direct flow paths. However, as the measured quantity in stack test is hydrogen leak rather than total leak, even if the leak was totally advective of nature, the hydrogen leak rate would increase as a function of hydrogen concentration in the gas which makes it difficult to draw the final conclusions. At nominal operating conditions of 0.25 A cm^{-2} current density, 46% fuel utilization and 20% air utilization the stack had a total hydrogen cross leak of 60 ml min^{-1}. The hydrogen cross leak value at nominal operating conditions corresponds to a loss of 0.7% of the inlet hydrogen flow, which can be considered a very promising result for the first test using coated Thermiculite 866 seals in a real SOFC stack.

Table 2
Nominal operating conditions.

Cells	30 pcs Elcogen ASC-10B
Flow configuration	Co-flow
Active area	81 cm^2
Cathode inlet temperature	590 °C
Cathode outlet temperature	700 °C
Current density	0.25 A cm^{-2}
Air utilization	22%
Fuel utilization	46%
Pressure difference over anode	3 mbar
Cathode inlet pressure	13 mbar
Cathode outlet pressure	Ambient

Table 3
Summary of the measurements and calculated cross leak rates at different operating conditions. The cathode inlet humidity was constant 0.08%.

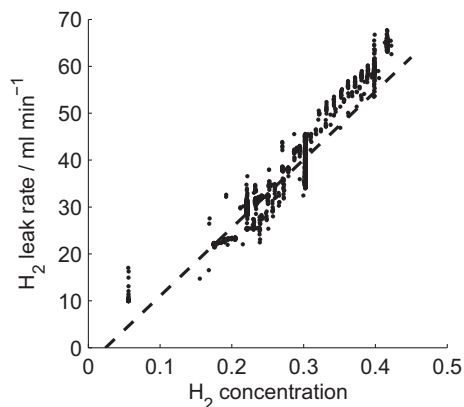|	Flow rate/ml min^{-1}			Measured quantity	Calculated cross leak/ml min^{-1}
	H_2	N_2	Air		
Before reduction	0	4500	4500	0.18% O_2 (anode out)	8 ± 2 (O_2)
Purge gas	500	8500	8500	0.20% H_2O (cathode out)	10 ± 2 (H_2)
Nominal	9000	8500	50,000	0.20% H_2O (cathode out)	60 ± 12 (H_2)

Fig. 7. Hydrogen cross leak as a function of average hydrogen concentration between anode inlet and outlet.

4. Conclusions

A coating method to deposit thin glass layers on compressible sealing materials was developed. Thermiculite 866 seals were coated with glass powder in organic carrier and were subsequently heat treated. The glass coating was conformable filling the surface imperfections of the Themiculite 866 core and the adjacent components effectively blocking interfacial leak paths. The coated Thermiculite 866 seals showed leak rates of 0.1–0.3 ml (m min)$^{-1}$, which is a reduction of 60–90% compared to uncoated samples which showed leak rates of 0.3–3 ml (m min)$^{-1}$. Leak rates of the coated seals as a function of overpressure were measured to be almost constant but very much dependent on the hydrogen concentration indicating that the coating effectively blocked the interfacial leak paths. The effect of gas composition to the leak rate should be considered carefully when comparing leak test results between different literature sources, as it can vary greatly.

A 30-cell stack was manufactured and tested to verify the feasibility of the coated seals in stack conditions. At nominal operating conditions of 0.25 A cm^{-2}, 46% fuel utilization and 20% air utilization the stack had a total hydrogen cross leak of 60 ml min^{-1} corresponding to 0.7% of the inlet hydrogen flow rate which can be considered a very promising result for the first stack test using these seals.

Acknowledgements

References

[1] J.W. Fergus, J. Power Sources 147 (2005) 46–57.
[2] P. Lessing, J. Mater. Sci. 42 (2007) 3465–3476.
[3] K. Weil, J. Miner. Metals Mater. Soc. (2006) 37–44.
[4] A. Shyam, R. Trejo, D. McGlurg, A. Ladoucceur, M. Kirkham, X. Song, J. Howe, E. Lara-Curzio, J. Mater. Sci. 48 (2013) 5880–5898.
[5] Y.S. Chou, J.W. Stevenson, L.A. Chick, J. Power Sources 112 (2002) 130–136.
[6] Y.S. Chou, J.W. Stevenson, L.A. Chick, J. Am. Ceram. Soc. 86 (2003) 1003–1007.
[7] M. Bram, S. Reckers, P. Drinovac, J. Mönch, R.W. Steinbrech, H.P. Buchkremer, D. Stöver, J. Power Sources 138 (2004) 111–119.
[8] S.P. Simner, J.W. Stevenson, J. Power Sources 102 (2001) 310–316.
[9] M. Rautanen, O. Himanen, V. Saarinen, J. Kiviaho, Fuel Cells (2009) 753–759.
[10] O. Thomann, M. Pihlatie, M. Rautanen, O. Himanen, J. Lagerbom, T. Varis, T. Suhonen, J. Kiviaho, J. Therm. Spray Technol. 22 (2013) 631–639.
[11] Y.S. Chou, J.W. Stevenson, J. Power Sources 191 (2009) 384–389.
[12] Y.S. Chou, J.W. Stevenson, Ceram. Trans. 161 (2005) 69–78.
[13] Y.S. Chou, J.W. Stevenson, J. Power Sources 157 (2006) 260–270.
[14] Y.S. Chou, J.W. Stevenson, J. Power Sources 135 (2004) 72–78.
[15] Y.S. Chou, J.W. Stevenson, P. Singh, J. Power Sources 152 (2005) 168–174.
[16] J. Hoyes, S. Bond, Sealing Technol. (2007) 11–14.
[17] Y.S. Chou, E.C. Thomsen, R.T. Williams, J.-P. Choi, N.L. Canfield, J.F. Bonnett, J.W. Stevenson, A. Shyam, E. Lara-Curzio, J. Power Sources 196 (2011) 2709–2716.